An integrated octree-RANSAC technique for automated LiDAR building data segmentation for decorative buildings

Fatemeh Hamid-Lakzaeian, Prof. Debra F. Laefer

School of Civil Engineering and Earth Institute, University College Dublin, Dublin, Ireland
fati.lakzaian@gmail.com, fatemeh.hamid-lakzaeian@ucdconnect.ie
debra.laefer@ucd.ie

Abstract. This paper introduces a new method for the automated segmentation of laser scanning data for decorative urban buildings. The method combines octree indexing and RANSAC - two previously established but heretofore not integrated techniques. The approach was successfully applied to terrestrial point clouds of the facades of five highly decorative urban structures for which existing approaches could not provide an automated pipeline. The segmentation technique was relatively efficient and wholly scalable requiring only 1 second per 1,000 points, regardless of the façade's level of ornamentation or non-rectilinearity. While the technique struggled with shallow protrusions, its ability to process a wide range of building types and opening shapes with data densities as low as 400 pts/m^2 demonstrate its inherent potential as part of a large and more sophisticated processing approach.

1 Introduction

Increasingly there is a need for accurate geometric representation of existing structures. This is true for many applications including heritage asset management [1], auto-navigation [2], and environmental analysis [3]. The challenge is to do so in a rapid and cost effective manner. Many researchers have demonstrated the capability to derive such models from laser scanning data [also known as Light Detection and Ranging (LiDAR). This remote sensing technique generates data comprised of individual points with x-, y-, and z- coordinates but with no inherently pre-defined relationship to each other. Therefore, one of the most important operations is segmentation, which is a critical step in most feature extraction tasks that ultimately define real objects within a point cloud. Notably, when encountering a complicated or non-planar façade, most existing feature extraction techniques are reliant upon manual intervention for this part or struggle to generate a high level of accuracy. This is often evident in automatic window identification, an important step for model reconstruction. To address this subject, the current work introduces a new, fully automated technique employing a combined octree and RANSAC to discern a building's principal façade from the window section planes for highly ornamented structures.

2 Research background

Identifying building openings has remained a major challenge in building reconstruction from remote sensing data (both LiDAR and imagery) in terms of producing accurate geometry. To achieve sufficient accuracy for window detection, the first step is often the segmenting of a point cloud in a systematic manner, so that the planes of openings versus that of the principal façade are detected properly. Some previous studies that have addressed window detection strategies are discussed herein.

As a fly-through rendering application for reconstructing three-dimensional (3D) windows, Lee and Nevatia [4] extracted 3D building models including recessed and protruded parts. The authors employed uncalibrated camera ground images and aligned them with two-dimensional (2D) building aerial image models. They used the horizontal and vertical pattern of window facades by applying a profile projection technique. Then, employing 2D information (i.e. width and height and image texture information), they classified openings. Windows were defined by size, appearance and shape. As part of this, they used an image-based refinement method for every candidate window using a one-dimensional search for the four sides of each opening. Finally integration of the reconstructed 3D window models with a larger 3D building model was performed. The accuracy level for the computed depths and ground truth data reported by the authors were within 8 cm.

Street-level geo-viewers were implemented by Haugeard et al. [5] to identify and detect the façade openings. By designing a kernel similarity function and the concept of graph matching on images, the researchers extracted each opening as a sub-graph from among a database of window images. To extract windows, they extended the work of Lee and Nevatia [4], which used geometric specifications of openings, as well as façade window arrays. Haugeard et al. [5] provided an example of a window query on a façade for correct opening classification based on the findings of the subgraph. They used two weighting techniques (scale and orientation) alongside their kernel method.

The work by Lee and Nevatia [4] was also extended by Recky and Leberl [6] who used gradient projection to detect different opening types on projected façade images – some with a high perspective distortion. As part of that, the façade was divided into row and column orientations by employing the concepts of gradient projection and local peaks. This enabled separator lines to be established. By applying thresholds on the horizontal projection identifiable levels set of blocks were created. Based on the position or gradient content, colour histograms as descriptors, as well as block size, they were able to categorize and label the various parts as either as solid façade or window. In experiments on façade images of buildings in Graz, Austria, a 22% improvement was claimed over a traditional gradient projection technique.

Subsequently Tuttas and Stilla [7] applied a Fourier Transform to interior building points captured during aerial LiDAR point clouds. In particular, regularities in the appearance of such data behind the façade planes were considered. Initially, they calculated the point normals and grouped the points using a region-growing concept. That was followed by applying RANSAC (as will be described subsequently) to detect the main façade and then the interior points. Fitting a Gaussian function to the histogram of the point distribution and

searching the repetitions in the structure by employing a Fourier Transform enabled window detection. Their approach was tested successfully on the large façades of the buildings of the Technical University Munich. Evaluation results were reported as a function of the number of windows identified but not their actual dimensions.

Shortly after that, Wang et al. [8] established a technique for window detection and window localization applied to mobile LiDAR data. In that work, they employed Principal Component Analysis (PCA) to calculate the surface normal, cluster the point clouds, and discover the possible façade. In order to fit the plane and extract the façade, they also implemented RANSAC and then a plane-sweep principle, where the rows and columns of window profile histograms were created. Consequently, the window sizes and spatial arrangements were extracted. Based on testing of 6 datasets, completeness and correctness consistently exceeded 70% and was as much as 100%. The authors noted that the technique was not currently suitable for non-planar buildings, non-rectilinear windows, or glass buildings where there were generally insufficient points on solid façade materials to process. To address the continued problem of non-planar and highly ornamented buildings, this paper introduces a new, fully automated approach, as described below.

3 Methodology

The proposed approach combines two existing techniques. The first is a well-known technique in computer vision to extract shapes entitled Random Sample Consensus (RANSAC) [9]. RANSAC is an iterative method to estimate parameters of a mathematical model from a set of observed data that contains outliers. Plane fitting is a common activity [10, 11 and 12]. The second technique is also one that has been used for LiDAR storage [13], processing and indexing [14, 15 and 16]. The octree indexing divides a space into eight cells and does this recursively, until a pre-specified threshold is met and all the points inside each bin are homogeneous or some other independently identified criterion is selected. In this work, every division or bin is called a volumetric cubical container (VCC). The summary of the technique developed is depicted in the flowchart (Fig. 1). Notably, what is unusual about the approach adopted below is that the RANSAC technique is embedded within the octree VCCs instead of first applying the RANSAC to generate an initial plane, as is commonly undertaken.

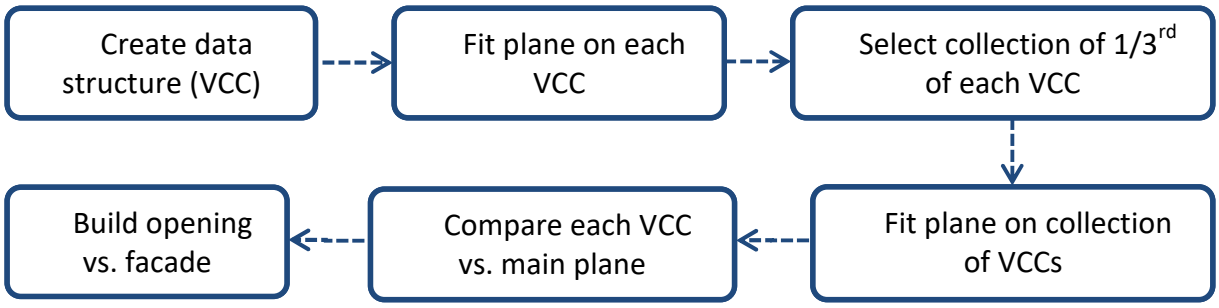

Fig. 1. Flowchart of the Octree-RANSAC algorithm

Since the initial laser scanning data are stored in a largely unorganized manner, the initial step must address data organization. An efficient processing method requires the implementation of a data structure, which can be achieved through imposition of an octree with a predefined, maximum capacity per VCC. Based on empirical trials, an upper limit of 200 points was selected as the terminal condition for each VCC. Once each VCC is established, RANSAC is applied within each one to fit the best possible plane to that small collection of points. The parameters that define the RANSAC calculation are the number of total points, the number of starting points (herein 3 randomly selected points), the number of iterations (herein 40 times based on trial and error), and a threshold distance between individual points to the fitted plane (herein selected as 1 cm based on construction practices and also remote sensing data acquisition). Each plane has a particular planar equation (equation 1) composed of the selected points. If the distance to an individual point does not exceed the distance threshold, the point is added to the selected points on the plane, and the plane is recalculated according to equation 1

$$a (x-x_0) + b (y-y_0) + c (z-z_0) = 0 \quad (1)$$

$$ax + by + cz + d = 0 \quad (2)$$

where a, b and c in equation 2 represent the components of normal vector, and x_0, y_0 and z_0 belong to a particular point on the plane. The output is an individual plane within each VCC. From amongst the 40 trials, the plane containing the largest number of points is the selected plane. The next step calculates the main plane of the façade using the original dataset in its entirety. One-third of the points are selected randomly from each VCC. Then RANSAC is applied across the entire collection of the selected points gathered from the VCCs. Next, 3 points are randomly selected, and the procedure is repeated for 100 iterations using a previously established threshold of 1 cm. The plane with the greatest percentage of affiliated points is then deemed the overall, main façade (plane).

Next, the plane of each VCC is checked against the main plane, by applying RANSAC once more, but this time with a 10 cm threshold. If the percentage of qualifying points exceeds 50%, then the VCC is co-planar with the main plane. Opening sections are detectable, as there are no data in those areas that are within the distance threshold (Fig.s 2-4).

3.1 Analysis and Results

To evaluate the validity of the above approach, five buildings were chosen as case studies to experimentally test the technique. Building selection was based on identifying multiple levels and types of façade ornamentation and non-rectilinear openings. The characteristics of the buildings are summarized in Table 1. Three buildings (1, 3, and 5) are located in Dublin's city centre along Grafton Street. The other two buildings (2 and 4) are located on Dublin's Southside: one within the researchers' campus (Building 2) and one in the nearby Richview office park (Building 4). While the buildings were selected to represent a range of structural and decorative complexities, Building 2 is notable due to its significant non-rectilinear openings and a highly complex roof structure. Building 4 is characterized by two different façade

materials (which differentiate the two stories) and has deep recesses along the horizontal plane of the principal façade, and Building 5 has various recesses along the main façade in the vertical direction. Data density ranged from quite low (391 pts/m^2 for Building 2) to nearly 2 orders of magnitude higher (16,181 pts/m^2 for Building 4). The façade areas that were processed ranged from 56.72 m^2 to 148.3 m^2 and came from as few as 2 scan stations to as many as 4.

Table 1. Features of Case Study buildings

Building	Façade Area (m^2)	Scan stations	Total points	Average density (pts/m^2)	Processing time (sec)
1	70.21	2	154,522	2,201	139
2	148.3	3	57,957	391	51
3	91.40	3	151,729	1,660	126
4	69.95	4	1,131,836	16,181	1,189
5	56.72	2	116,110	2,047	101

For the Buildings 1, 2, and 3 (Table 1), the patches created and the façade versus openings displayed are shown in Fig.s 2-4. In Building 1 (Fig. 2), the roofline level (identified in red) that protruded from the principal facade was not detected as a part of the main façade (displayed in blue); however the opening sections were properly distinguished from the principal façade.

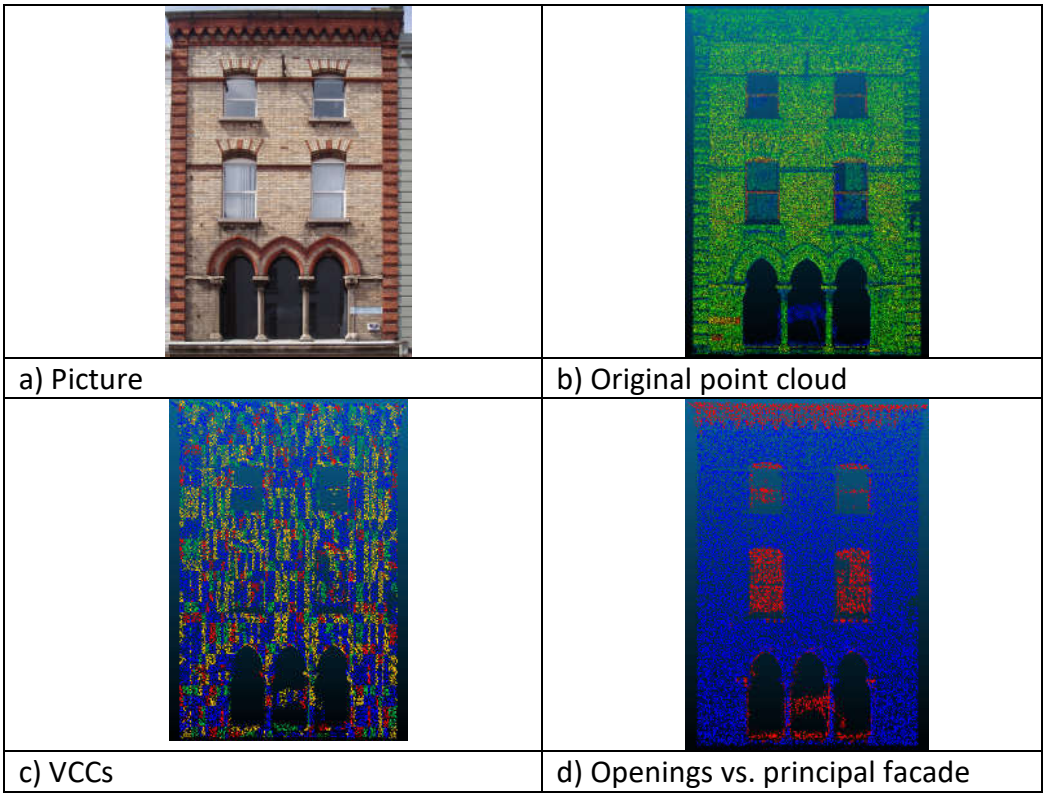

a) Picture | b) Original point cloud

c) VCCs | d) Openings vs. principal facade

Fig. 2. Recess vs. principal facade detection; 42 Grafton (Building 1)

a) Picture | b) Original point cloud

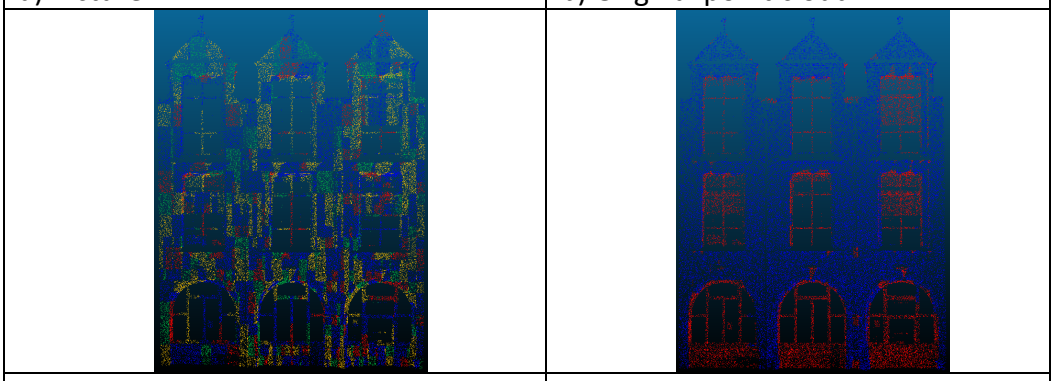

c) VCCs | d) Openings vs. principal facade

Fig. 3. Recess vs. principal facade detection; UCD School of Architecture (Building 2)

There are some architectural features in Building 2 that were detected on the triangular-shape of the roofline and also the top level of the openings on the ground floor (shown in red). Those minor sections protruded from the main plane of the façade making them difficult to detect (Fig. 3).

a) Picture | b) Original point cloud

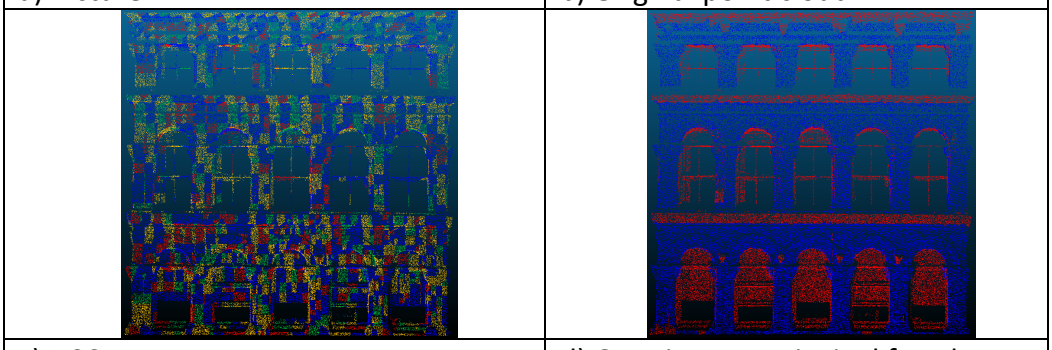

c) VCCs | d) Openings vs. principal facade

Fig. 4. Recess vs. principal facade detection; 24 Grafton (Building 3)

The story levels of the structure in Building 3 that protruded significantly from the main façade were not detected as co-planar with the main plane of the façade. Also, secondary architectural elements on the roof level and between windows on the lower story that protruded from principal façade were not merged with the main plane, while major façade and openings were detected correctly (Fig. 4).

3.2 Discussion

Most of the 5 buildings were similarly sized (between 56.72 to 91.40 m^2), except Building 2, which had an area of 148.3 m^2. The buildings required similar computational resources (between 51 sec to 139 sec), except for Building 4 with its 4 scan stations and a point count more than an order of magnitude over the other buildings. This required 1,189 seconds. As shown in Fig. 5, the processing time is highly linear, irrespective of the façade's complexity or façade area being processed. Only the point count is driving the processing time.

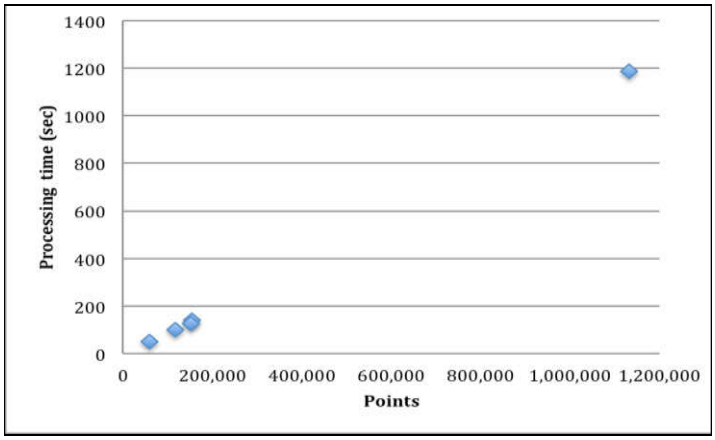

Fig. 5. Demonstration of the no. of points versus processing time (sec) for five case studies

Several experiments from different case studies demonstrated conclusively the ability to discern recesses in a façade and multiple planes, irrespective of layout or orientation. Where problems arose was in the pairing of various sections of facades that should be continuous but had relatively shallow decorative protrusions. In such instances (Fig.s 6 and 7), the structure of the planes to represent the main facade and plane of openings, while successfully segmented were not reconstructed as expected. For example with Building 4, the algorithm generated two facades instead of one with a protrusion. In this case (Fig. 6d) there is a seeming reversal of the planes. Specifically, the openings on ground floor was identified in blue with red as the colour for the principal façade, while on the first floor, the colours were reversed. The reconstruction for Building 5 exhibited similar difficulties. Despite the opening planes being detected consistently for the first and second floors, the existence of the recess in the vertical direction (i.e. the columns between the openings) caused the principal façade to be ultimately misclassified into two sections (Fig. 7d).

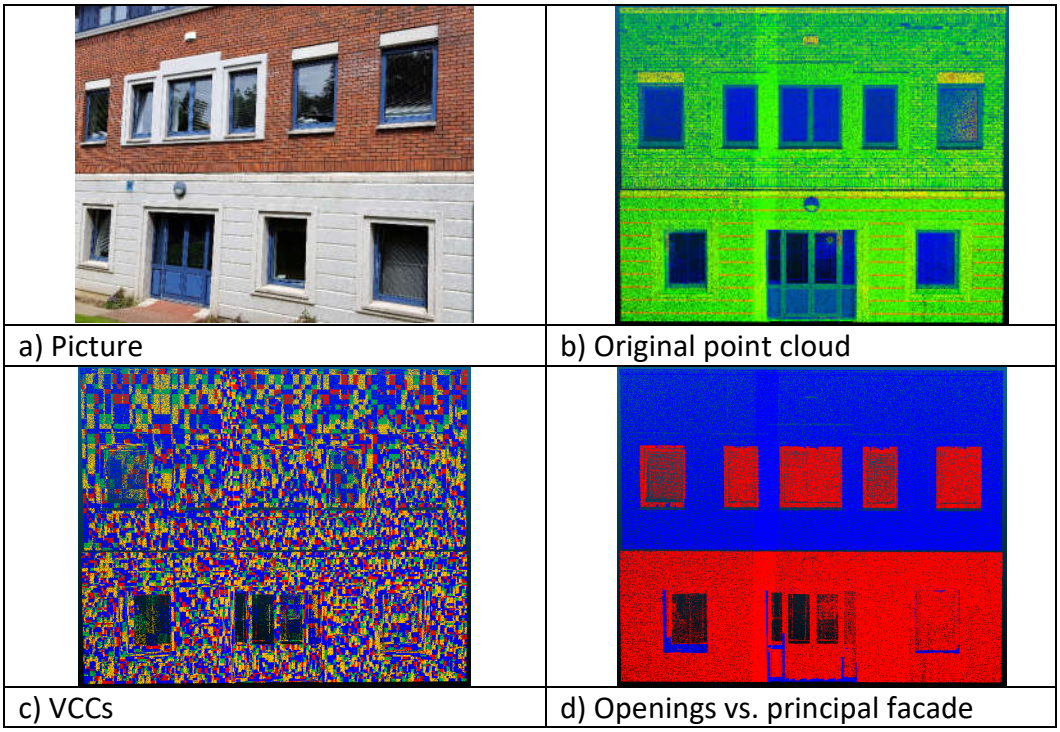

a) Picture | b) Original point cloud

c) VCCs | d) Openings vs. principal facade

Fig. 6. Recess vs. principal facade display, Failure on horizontal recess detection; Unit 9 Rich-view (Building 4)

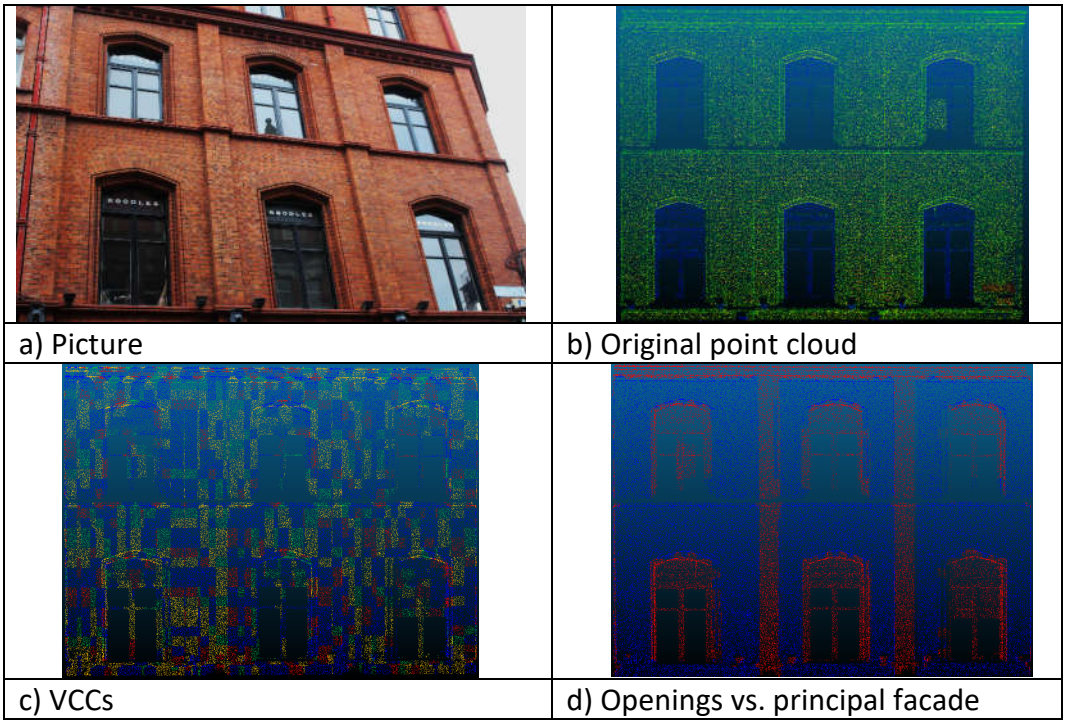

a) Picture | b) Original point cloud

c) VCCs | d) Openings vs. principal facade

Fig. 7. Recess vs. principal facade display, failure on vertical recess detection; 71 Grafton (Building 5)

While difficulties in the ultimate correct segmentation of façades with relatively shallow protrusions denote that further refinement of this approach is needed, the scalability and visually convincing outcomes of the technique (Buildings 1-3) point to the underlying potential of the approach. Of particular note was the ability to successfully process non-rectilinear

openings at quite low point densities such as in the case of Building 2 where the point density was below 400 pts/m^2.

4 Conclusions

To reduce the processing time while computing different planar objects on the façade and detecting the building features, the point cloud data were organized employing an octree structure. Subsequently, a modified RANSAC algorithm was embedded within the lowest component along each octree branch. The technique was able to differentiate between the planes of openings and the principal façade for highly non-rectilinear and ornamented buildings. The novelty of this approach is (1) in the embedding of RANSAC within each volumetric cubical container created by an octree index to segregate the principal plane of the façade from opening recesses and then (2) in the reconstruction of the larger planes through a distance criterion. This involves specialized parameter selection to successfully distinguish co-planar elements from parallel ones.

This approach generated segmentation times of approximately 1 second per 1,000 points wholly irrespective of the façade's geometric or decorative complexity. While further work is needed on final classification means, the robustness of the technique with respect to building types and complexities, its scalability with large dataset sizes, and its ability to succeed at relatively low point densities, shows the strong inherent value of this line of research.

Acknowledgments

This work was generously funded by the European Research Council grant ERC-2012-StG-20111012 'RETURN-Rethinking Tunnelling in Urban Neighbourhoods' Project 307836. The authors gratefully thank Donal Lennon for the pre-processing of the data sets, as well as for assistance with data acquisition.

References

1. Zolanvari, S., Laefer, D.F., 2016. Slicing Method for Building Facade Extraction from LiDAR Point Clouds. ISPRS 119(Sept) pp. 334-346.
2. Vo, A.-V., Truong-Hong, L., Laefer, D.F., Tiede, S. d'Oleire-Oltmanns, A., Baraldi, Shimoni, M., Moser, G. Tuia, D. 2016. Processing of Extremely High Resolution LiDAR and RGB Data: Outcome of the 2015 IEEE GRSS Data Fusion Contest —Part B: 3-D Contest. Journal of Selected Topics in Applied Earth Observations and Remote Sensing, 99 (Aug) pp. 1-16.
3. Singh, M., Laefer, D.F. 2015. Recent Trends and Remaining Limitations in Urban Microclimate Models." Open Urban Studies and Demographics Journal, 1(1) pp.1-12.
4. Lee, S.C. and Nevatia, R., 2004, June. Extraction and integration of window in a 3D building model from ground view images. In Computer Vision and Pattern Recognition, 2004. CVPR 2004. Proceedings of the 2004 IEEE Computer Society Conference on (Vol. 2, pp. II-113). IEEE.

5. Haugeard, J.E., Philipp-Foliguet, S. and Precioso, F., 2009, November. Windows and facades retrieval using similarity on graph of contours. In 2009 16th IEEE International Conference on Image Processing (ICIP) (pp. 269-272). IEEE.
6. Recky, M. and Leberl, F., 2010, July. Window detection in complex facades. In Visual Information Processing (EUVIP), 2010 2nd European Workshop on (pp. 220-225). IEEE.
7. Tuttas, S. and Stilla, U., 2011. Window detection in sparse point clouds using indoor points. International Archives of Photogrammetry, Remote Sensing and Spatial Information Sciences, 38, p.3.
8. Wang, R., Ferrie, F.P. and Macfarlane, J., 2012. A method for detecting windows from mobile LiDAR data. Photogrammetric Engineering & Remote Sensing, 78(11), pp.1129-1140.
9. Fischler, M.A. and Bolles, R.C., 1981. Random sample consensus: a paradigm for model fitting with applications to image analysis and automated cartography. Communications of the ACM, 24(6), pp.381-395.
10. Yang, M.Y. and Förstner, W., 2010, January. Plane detection in point cloud data. In Proceedings of the 2nd in Conference on Machine Control Guidance, Bonn (Vol. 1, pp. 95-104).
11. Oehler, B., Stueckler, J., Welle, J., Schulz, D. and Behnke, S., 2011, December. Efficient multi-resolution plane segmentation of 3d point clouds. In International Conference on Intelligent Robotics and Applications (pp. 145-156). Springer Berlin Heidelberg.
12. Awwad, T.M., Zhu, Q., Du, Z. and Zhang, Y., 2010. An improved segmentation approach for planar surfaces from unstructured 3D point clouds. The Photogrammetric Record, 25(129), pp.5-23.
13. Mosa, A.S.M., Schön, B., Bertolotto, M. and Laefer, D.F., 2012. Evaluating the benefits of octree-based indexing for LiDAR data. Photogrammetric Engineering & Remote Sensing, 78(9), pp.927-934.
14. Truong-Hong, L. and Laefer, D.F., 2014. Octree-based, automatic building facade generation from LiDAR data. Computer-Aided Design, 53, pp.46-61.
15. Bucksch, A. and Lindenbergh, R., 2008. CAMPINO—A skeletonization method for point cloud processing. ISPRS journal of photogrammetry and remote sensing, 63(1), pp.115-127.
16. Wang, M. and Tseng, Y.H., 2011. Incremental segmentation of lidar point clouds with an octree-structured voxel space. The Photogrammetric Record, 26(133), pp.32-57.